IOSR Journal of Applied Physics (IOSR-JAP)
e-ISSN: 2278-4861.Volume 11, Issue 4 Ser. I (Jul. – Aug. 2019), PP 26-30
www.iosrjournals.org

$MoSe_2/ZrSe_2$ van der Waals Heterostructure Tunneling Field-Effect Transistor with Substitutional Doped Source

Wen-Lun Zhang[1]

[1]*Department of Electrical and Electronic Engineering, Tokyo Institute of Technology, Tokyo 152-8552, Japan*
Corresponding Author: Wen-Lun Zhang

Abstract: *This research details the experimental results of $MoSe_2/ZrSe_2$ van der Waals (vdW) heterostructure tunneling field-effect transistor (TFET) using Ti-doped $MoSe_2$ as source material. The electrical characteristics of $MoSe_2$ metal-oxide-semiconductor field-effect transistors were investigated and the Ti doped $MoSe_2$ exhibited strong p-type conduction. The fabricated $MoSe_2/ZrSe_2$ vdW heterostructure TFET successfully implemented transistor operation, and the asymmetrical diode properties manifested that the band alignment of the $MoSe_2/ZrSe_2$ vdW heterostructure TFET could be modulated from Type-II to Type-III by the back-gate bias. These results verified that the Ti-doped $MoSe_2$ is an appropriate p-type two-dimensional material for designing vdW heterostructure TFET.*

Keywords: *Two-dimensional materials, Tunneling field-effect transistor, Molybdenum diselenide, Zirconium diselenide, Substitutional doping*

Date of Submission: 25-06-2019 Date of acceptance: 12-07-2019

I. Introduction

Miniaturization of the semiconductor devices activated the evolution of the electronics industry by scaling down the dimension of transistors. Despite of the improvement on electrical performance of metal-oxide-semiconductor field-effect transistors (MOSFETs) by the rule of scaling, the increasing power consumption is becoming a critical problem to be solved. Although a scaled operating voltage, V_{DD}, can drastically reduce the power dissipation of the integrated circuit, the subthreshold swing (SS) of a traditional MOSFET is not scalable and has a minimum of 60 mV/dec at room temperature, which is physically limited by the thermal tail of Boltzmann distribution. To break the 60 mV/dec limitation and further scale down the V_{DD}, it is necessary to develop novel transistors with different turn-on mechanism. Tunneling field-effect transistor (TFET), [1] whose carrier injection originated by quantum mechanical band-to-band tunneling (BTBT), is a promising competitive candidate for subthermionic operation in future power-efficient electronics. Some milestones of research on TFETs had been set for the successful realization of sub-60 mV/dec or high on-current operation. [2] However, TFETs exhibiting both steep slope and high current operation that satisfy the International Technology Roadmap for Semiconductors has not been explored. One confinement of conventional bulk materials is degraded electron mobility as scaled to a low dimensional film, which restricts high speed operation of the TFET. Also, the imperfections and trap states at the tunneling junction significantly deteriorate the gate controllability, which gives rise to increased SS. [3] Thus, development of novel material towards the More Moore technology booster is essential for high performance TFET implementation. Transition metal dichalcogenides (TMDs) are two-dimensional (2D) materials with both reasonable electron mobility and finite bandgap, showing promise for applications in electronic industry as candidates of next-generation materials. [4-5] Various band alignments of TFETs can be easily designed by stacking one TMD material onto another without considering lattice mismatch. [6] Furthermore, large tunneling interface with low trap density can be obtained in 2D-2D TFETs due to their pristine surface. Some attempts on fabrication of TMDs based TFET successfully realized high performance operation, [7-9] but the p-type source in TMD material always contains atom diffusion and charge transfer by oxidation, which is not controllable. [10] Black phosphorus, an intrinsic p-type 2D semiconductor, is available choice for 2D source material but is sensitive in air, which is difficult for practical application. [11] Therefore, a stable substitutional p-type source TMD material with controllable hole concentration is highly desirable for 2D-2D TFETs. In this study, $MoSe_2$ doped with Ti was investigated as a potential source material in 2D-2D TFETs. Moreover, a $MoSe_2/ZrSe_2$ van der Waals (vdW) heterostructure TFET was fabricated to characterize the electrical performance of TFET using Ti-doped $MoSe_2$ as source, laying evidence that the Ti-doped $MoSe_2$ is suitable for 2D-2D TFET implementation.

II. Device Fabrication

First, 20 nm of HfO_2 was formed on p^{++}-Si substrate by 200 cycles of atomic layer deposition (ALD) using tetrakis(dimethylamino)hafnium (TDMAH) and H_2O at 250°C as back-gate dielectric. The $ZrSe_2$ flakes were mechanically exfoliated by scotch-tape and randomly transferred onto the substrate. Relatively thin $ZrSe_2$ flakes were located on the substrate as channel for vdW heterostructure TFET. Ti-doped $MoSe_2$ flakes were exfoliated simultaneously and transferred onto polydimethylsiloxane (PDMS), and then overlapped with objective $ZrSe_2$ flake to fabricate a vdW heterostructure via viscoelastic stamping method using a micromanipulation system. [12] The doping level (Ti) of $MoSe_2$ was approximately 10^{21} cm^{-3} without band renormalization, and the $MoSe_2$ and $ZrSe_2$ crystals were commercial merchandise from 2Dsemiconductor, Inc. After the dry transferring of p-type $MoSe_2$ as source of TFET, S/D electrodes were designed for both $MoSe_2$ and $ZrSe_2$ flakes to investigate the electrical performance respectively by electron beam lithography. Ni/Au (20 nm/80 nm) was deposited on the substrate by electron beam evaporation and followed by a standard lift-off process, then a 20 nm of HfO_2 was deposited on the substrate as a passivation layer via 200 cycle ALD of TDMAH and H_2O at 250°C, protecting the vdW heterostructure TFET from ambient contamination. Finally, Cr/Au (20 nm/100 nm) was deposited as back contact by electron beam evaporation, and the device was accomplished after dry etching S/D contact holes. $MoSe_2$ MOSFETs were also fabricated to confirm the p-type transistor conduction via similar process flow.

III. Results And Discussions

The effect of Ti-doping on the electrical characteristics was investigated as shown in Fig. 1. $MoSe_2$ MOSFET without Ti doping was fabricated and the transfer curves were shown in Fig. 1 (a). The pristine $MoSe_2$ MOSFET exhibited ambipolar transportation, and the n-type conduction was stronger than the p-type conduction, which is in accord with other experiment reports. [13] In comparison, the fabricated Ti-doped $MoSe_2$ MOSFET exhibited strong p-type conduction. Although the Ti-doped $MoSe_2$ MOSFET was biased at a relatively high positive gate voltage, the hole could not be fully depleted and the channel current of the transistor was larger than 10 nA. There was no current recovery for the electron accumulation observed in the Ti-doped $MoSe_2$ MOSFET, which indicated that the $MoSe_2$ was degenerately p-doped. The Ti-doped $MoSe_2$ was very stable in ambient, and the transfer curves did not shift even after 1 week of air exposure, which verified that the Ti-doped $MoSe_2$ is suitable for vdW heterostructure TFET.

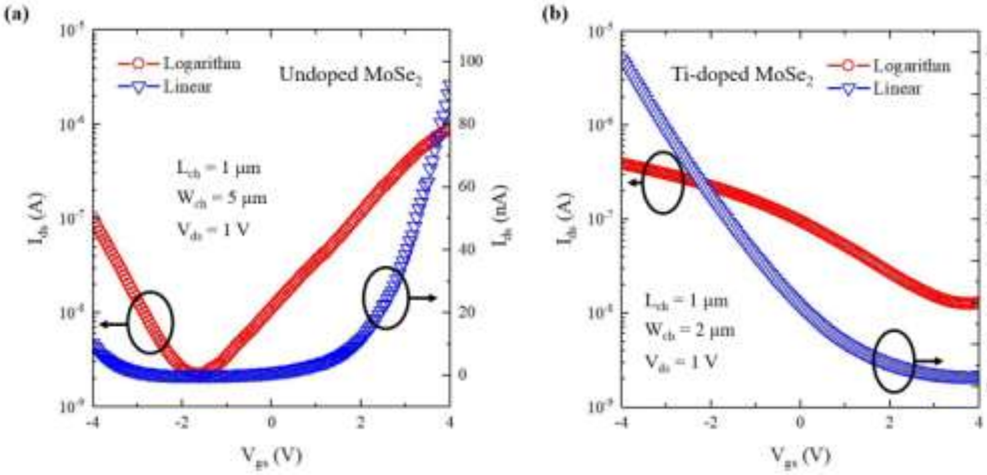

Figure 1. Transfer curves of $MoSe_2$ MOSFET before and after Ti-doping. The doping level was approximately 10^{21} cm^{-3}, the contact metal is Ni, and the gate dielectric was 20 nm HfO_2. **(a)** Transfer curves before Ti-doping. Ambipolar transport was observed in the transistor, and the n-type conduction was stronger than p-type conduction. **(b)** Transfer curves after Ti-doping. The $MoSe_2$ MOSFET exhibited strong p-type conduction without current recovery even the gate bias exceeded 4 V, which confirmed the degenerately p-doping concentration.

After confirming the p-type conduction of the Ti-doped $MoSe_2$, the fabricated $MoSe_2$/$ZrSe_2$ vdW heterostructure TFET was characterized. Fig. 2 (a) depicts the schematic view of the fabricated device, and Fig. 2 (b) is the optical microscope image. The $MoSe_2$/$ZrSe_2$ vdW heterostructure area was also analyzed by atomic force microscopy (AFM) and the results were shown in Fig. 3 (c). The flake thickness along the red dotted line ($MoSe_2$) and green dotted line ($ZrSe_2$) was 21 nm and 16 nm, respectively. The cross-section of the vdW heterostructure along the green dotted line in Fig. 2 (b) was characterized by transmission electron microscopy

(TEM) and the image was shown in Fig. 2 (d). The flake thickness of $MoSe_2$ and $ZrSe_2$ was in accord with the scanning result of AFM. The elementary composition of the vdW heterostructure area was mapped via energy dispersive X-ray spectrometry (EDX) and the results were shown in Fig. 2 (e), which verified that the vdW heterostructure TFET was constructed by HfO_2 gate dielectric, Ti-doped $MoSe_2$, and $ZrSe_2$. The large vertical tunneling junction area and sharp interface thanks to stacking 2D materials were highly desired for high performance TFET, which is difficult to be realized in conventional bulk materials.

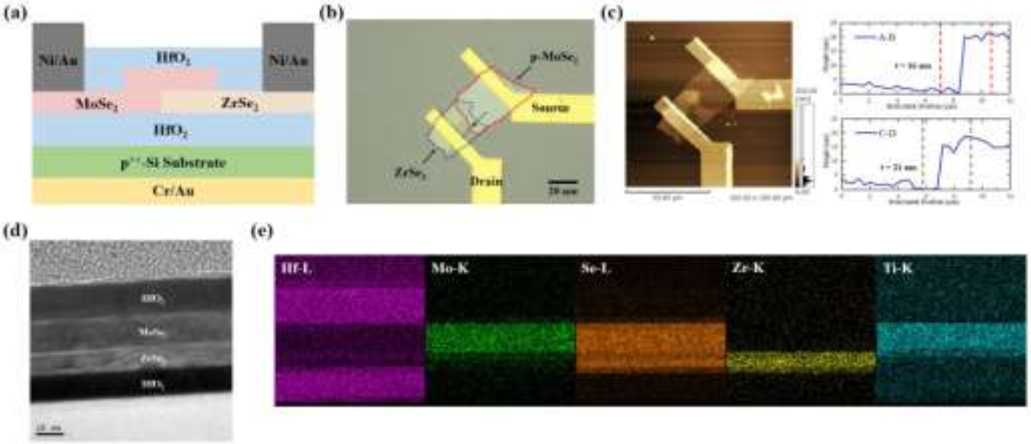

Figure 2. Device structure of fabricated $MoSe_2$/$ZrSe_2$ vdW heterostructure TFET. **(a)** Schematic view. **(b)** Optical microscope image. **(c)** AFM image and flake thickness. The red dotted line is defined as A-B ($ZrSe_2$) and the green dotted line as C-D ($MoSe_2$). The thickness of $MoSe_2$ and $ZrSe_2$ flakes were 21 nm and 16 nm, respectively. **(d)** TEM cross-section image of the $MoSe_2$/$ZrSe_2$ vdW heterostructure along the green dotted line in (b). **(e)** EDX mapping of the elementary composition of the $MoSe_2$/$ZrSe_2$ vdW heterostructure in Hf-L, Mo-K, Se-L, Zr-K, Ti-K, respectively.

In this paper, the $ZrSe_2$ was selected to the channel 2D material because of its relatively deep electron affinity and "native" ZrO_x oxide. [14] The valence band maximum of the $MoSe_2$ is at -5.23 eV and the conduction band minimum of the $ZrSe_2$ is at -5.86 eV by density function theory calculation, [15] so that the $MoSe_2$/$ZrSe_2$ vdW heterostructure system formed a Type-III broken band alignment.

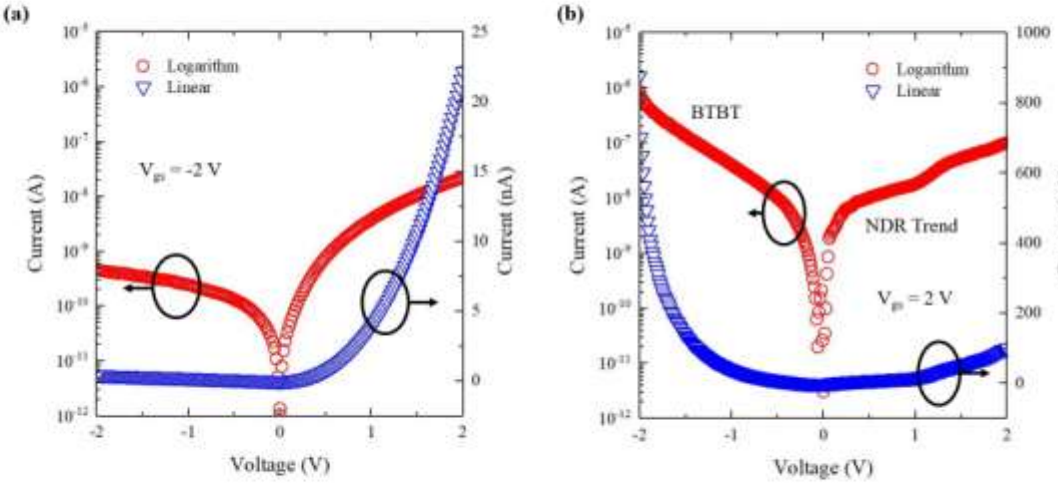

Figure 3. Electrical characteristics of fabricated $MoSe_2$/$ZrSe_2$ vdW heterostructure TFET as back-gate modulated diode. **(a)** Rectified characteristics measured at V_{gs} = -2 V and the band alignment of the heterostructure system was Type-II. **(b)** Tunneling characteristics and a trend towards NDR measured at V_{gs} = 2 V and the band alignment of the heterostructure system was Type-III.

To verify the calculation results, the p-$MoSe_2$/$ZrSe_2$ vdW heterostructure TFET was characterized as a back-gate modulated diode as shown in Fig. 3. When the back-gate bias was -2 V, the electrons in the $ZrSe_2$ channel were depleted, tuning the Fermi level of the $ZrSe_2$ channel closer to the valence band, switching the vdW heterostructure system into a Type-II staggered band alignment. As shown in Fig. 3 (a), when a positive voltage was biased at the $MoSe_2$ side, the potential barrier for the limited electrons in the $ZrSe_2$ channel was lowered and the electrons started diffusing to the $MoSe_2$ side. One the other hand, when the $MoSe_2$ terminal was biased negatively, only a small current flowed as reserve current of a p-n diode. The asymmetrical diode conduction manifested that the system was in a Type-II band alignment. The modulation of the band alignment from Type-II to Type-III could be verified in I-V characteristics of the tunneling diode characteristics at V_{gs} = 2 V as shown in Fig. 3 (b). A significantly increasing of the backward current was observed when the back-gate bias was turned to 2 V, which was originated by BTBT. In the forward current from 0 to 2 V, a trend towards the negative differential resistance (NDR) could be observed at room temperature, which proved that the heterostructure system was switched to a Type-III band alignment and the Ti-doped $MoSe_2$ was exactly degenerately p-doped. Thus, it could be estimated that a clearer NDR could be observed at low temperature.

After measuring the diode characteristics of the fabricated heterostructure, the transfer curves of the fabricated $MoSe_2$/$ZrSe_2$ vdW heterostructure TFET were investigated in Fig. 4 (a). The on/off ratio of the vdW heterostructure TFET was approximately 10^2, along with an 8 μA-on current at 1 V drain bias. Although the $MoSe_2$/$ZrSe_2$ vdW heterostructure TFET implemented basic operation of an electrical switch, the poor controllability of the TFET gave rise to large SS and insufficient on/off ratio, which was attributed to the poor performance of $ZrSe_2$ MOSFET. To illustrate this viewpoint, the transfer curves of a $ZrSe_2$ MOSFET fabricated on the same substrate were shown in Fig. 4 (b). The on/off ratio of the sample $ZrSe_2$ MOSFET did not exceed 10^3, along with a large SS over 1 V/dec. This is possibly due to the poor back-gate semiconductor/insulator interface between $ZrSe_2$ and HfO_2. [16] Also, the imperfection of the $ZrSe_2$ crystal restricted the performance of the vdW TFET.

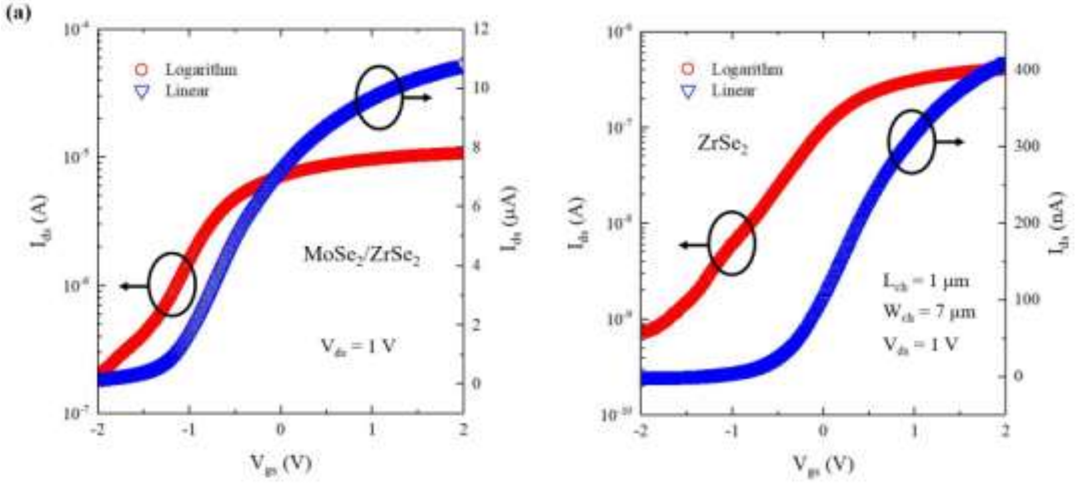

Figure 4. (a) Transfer curves of the fabricated $MoSe_2$/$ZrSe_2$ vdW heterostructure TFET at V_{ds} = 1 V. **(b)** Transfer curves of the $ZrSe_2$ MOSFET at V_{ds} = 1 V.

IV. Conclusion

This paper discussed the experimental results of $MoSe_2$/$ZrSe_2$ vdW heterostructure TFET using the Ti-doped $MoSe_2$ as source material. The pristine $MoSe_2$ exhibited stronger n-type ambipolar current conduction, while the $MoSe_2$ with Ti-doping exhibited degenerate p-type conduction. The fabricated $MoSe_2$/$ZrSe_2$ vdW heterostructure TFET implemented the transistor operation, and a trend towards NDR verified that the turn-on mechanism of the transistor originated by BTBT. Although the TFET did not realize steep-slope operation, the performance could be improved through optimizing the semiconductor/insulator interface and crystal qualities.

Acknowledgements

This work was supported by JSPS KAKENHI Grant Number JP18K04279.

References

[1]. A. M. Ionescu and H. Riel, Tunnel field-effect transistors as energy-efficient electronic switches, *Nature, 479*, 2011, 329-337.

[2]. E. Memisevic, J. Svensson, E. lind, and L.-E. Wernersson, Vertical Nanowire TFETs With Channel Diameter Down to 10 nm and Point S_{MIN} of 35 mV/Decade, *IEEE Electron Device Letters, 39(7)*, 2018, 1089-1091.

[3]. S. Agarwal and E. Yablonovitch, Band-Edge Steepness Obtained From Esaki/Backward Diode Current-Voltage Characteristics, *IEEE Transactions on Electron Devices, 61(5)*, 2014, 1488-1493.

[4]. B. Radisavljevic, A. Radenovic, J. Brivio, V. Giacometti, and A. Kis, Single-layer MoS2 transistors, *Nature Nanotechnology, 6*, 2011, 147-150.

[5]. W.-L. Zhang, Improvement of Performance of HfS_2 Transistors Using a Self-Assembled Monolayer as Gate Dielectric, *Chinese Physics Letters, 36(6)*, 2019, 067301.

[6]. A. K. Geim and I. V. Grigorieva, Van der Waals heterostructures, *Nature, 499*, 2013, 419-425.

[7]. X. Yan, C. Liu, C. Li, W. Bao, S. Ding, D. W. Zhang, and P. Zhou, Tunable $SnSe_2/WSe_2$ Heterostructure Tunneling Field Effect Transistor, *Small, 13*, 2017, 1701478.

[8]. P. Wu and J. Appenzeller, Reconfigurable Black Phosphorus Vertical Tunneling Field-Effect Transistor With Record High ON-Currents, *IEEE Electron Device Letters, 40(6)*, 2019, 981-984.

[9]. W. Zhang, T. Kanazawa, and Y. Miyamoto, Performance improvement of a p-MoS_2/HfS_2 van der Waals heterostructure tunneling FET by UV-O_3 treatment, *Applied Physics Express, 12(6)*, 2019, 065005.

[10]. J. He, N. Fang, K. Nakamura, K. Ueno, T. Taniguchi, K. Watanabe, and K. Nagashio, 2D Tunnel Field Effect Transistors (FETs) with a Stable Charge-Transfer-Type p^+-WSe_2 Source, *Advanced Electronic Materials, 4*, 2018, 1800207.

[11]. L. Li, Y. Yu, G. J. Ye, Q. Ge, X. Ou, H. Wu, D. Feng, X. H. Chen, and Y. Zhang, Black phosphorus field-effect transistors, *Nature Nanotechnology, 9*, 2014, 372-377.

[12]. A. Castellanos-Gomez, M. Buscema, R. Molenaar, V. Singh, L. Janssen, H. S J van der Zant, and G. A Steele, Deterministic transfer of two-dimensional materials by all-dry viscoelastic stamping, *2D Materials, 1*, 011002.

[13]. D. N. Ortiz, I. Ramos, N. J. Pinto, M.-Q. Zhao, V. Kumar, and A. T. Johnson, Ambipolar transport in CVD grown $MoSe_2$ monolayer using an ionic liquid gel gate dielectric, *AIP Advances, 8*, 2018, 035014.

[14]. M. J. Mleczko, C. Zhang, H. R. Lee, H.-H. Kuo, B. Magyari-Kope, R. G. Moore, Z.-X. Shen, I. R. Fisher, Y. Nishi, and E. Pop, $HfSe_2$ and $ZrSe_2$: Two-dimensional semiconductors with native high-k oxides, *Science Advances, 3(8)*, 2017, e1700481.

[15]. C. Gong, H. Zhang, W. Wang, L. Colombo, R. M. Wallace, and K. Cho, Band alignment of two-dimensional transition metal dichalcogenides: Application in tunnel field effect transistors, *Applied Physics Letters, 103(5)*, 2013, 053513.

[16]. W. Zhang, S. Netsu, T. Kanazawa, T. Amemiya, and Y. Miyamoto, Effect of increasing gate capacitance on the performance of a p-MoS_2/HfS_2 van der Waals heterostructure tunneling field-effect transistor, *Japanese Journal of Applied Physics, 58(SB)*, 2019, SBBH02.

Wen-Lun Zhang " MoSe2/ZrSe2 van der Waals Heterostructure Tunneling Field-Effect Transistor with Substitutional Doped Source.” IOSR Journal of Applied Physics (IOSR-JAP) , vol. 11, no. 4, 2019, pp. 26-30